"lock" the direction of the fish, only allowing the forward movement.

Without a sensor to feed the forward speed back in real time, experiments of turning while swimming forward or removing the yellow rope to carry out real experiment of in-situ turning are currently unavailable. In addition, there are no pectoral fins on the robotic fish so that the forward speed cannot be fully decoupled from the turning angle rate.

On the other hand, the control of the joint angle is still open-loop, i.e., the PWM control of the servomotors has no feedback. When high rotating rate is required, the real joint angles of the servo motors cannot be regarded the same as the output any more. Therefore a feedback of joint angles should also be incorporated into the control laws so that the control quality can be further enhanced. Also, high rotating rate can introduce other problems, such as unignorable coriolis forces, more complex nonlinearity, etc. These should be well considered in order to achieve better performances. However, under the limitation of most servomotors, the robotic fish can hardly obtain a turning rate faster than $200^\circ/s$, which yields only a little unwanted complexity.

IV. Conclusions and Future Work

In this paper we first divide the process of turning maneuver into three phases based on the fundamental functions of each phase, and then propose the closed-loop control method. This method provides a fast and precise control of the fish direction. With emphasis on the unbending phase, the key point of precise turning control is uncovered. Finally, experiments of in-situ turning are carried out, which offer a vivid verification to the proposed theories.

In the near future, we will replace the gyro by a wide-range one, and build new fish covering to broaden the range of the rotation of each joint, and import new sensors to perceive the linear speed. New control algorithms including the feedback of joint angles will also be investigated. As a plus, pectoral fins will be fixed on the robotic fish, so that we can fulfill the precise control, not only for turning maneuvers, but also for the site-specific tasks.

References

[1] P. R. Bandyopadhyay, "Trends in biorobotic autonomous undersea vehicles," *IEEE J. Ocean. Eng.*, vol. 30, no. 1, pp. 109-139, 2005.

[2] K. A. Morgansen, B. I. Triplett, and D. J. Klein, "Geometric methods for modeling and control of free-swimming fin-actuated underwater vehicles," *IEEE Trans. Robot.*, vol. 23, no. 6, pp. 1184–1199, 2007.

[3] J. Yu, L. Liu, L. Wang, M. Tan, and D. Xu, "Turning control of a multilink biomimetic robotic fish," *IEEE Trans. Robot.*, vol. 24, no. 1, pp. 201–206, Feb. 2008.

[4] J. Yu, M. Tan, S. Wang, and E. Chen, "Development of a biomimetic robotic fish and its control algorithm," *IEEE Trans. Syst. Man Cybern. B, Cybern.*, 34(4): 1798–1810, 2004.

[5] A. J. Ijspeert, A. Crespi, D. Ryczko, J.-M. Cabelguen, "From swimming to walking with a salamander robot driven by a spinal cord model," *Sci.*, vol. 315, pp. 1416–1419, 2007.

[6] K. A. McIsaac and J. P. Ostrowski, "Open-loop verification of motion planning for an underwater eel-like robot," *Experimental Robotics VII*, LNCIS 271, 2001, pp. 271–280.

[7] C. Zhou and K. H. Low, "Locomotion planning of biomimetic robotic fish with multi-joint actuation," in *Proc. IEEE Int. Conf. Intell. Robot. Syst.*, St. Louis, MO, USA, Oct. 2009, pp. 2132–2137.

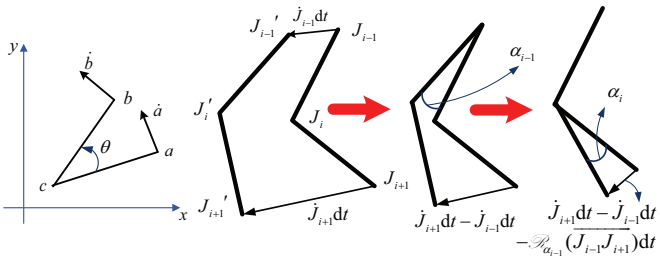

Fig. 9. (a) Illustration of the rotation transformation $\mathscr{S}_\theta$ from point a to b. $\dot{a}$ and $\dot{b}$ are the velocity vectors of a and b respectively. (b) The computation of the angle rate α_i, where $\dot{J}_{i-1}$, $\dot{J}_{i+1}$ and α_{i-1} is given.

[8] R. W. Blake, "Fish functional design and swimming performance," *J. Fish Biol.*, vol. 65, pp. 1193–1222, 2004.

[9] J. Yu, M. Wang, M. Tan, and Y. F. Li, "Step function based turning maneuvers in biomimetic robotic fish," in *Proc. IEEE Int. Conf. Robot. Autom.*, Kobe, Japan, May 2009, pp. 3431–3436.

[10] Q. Hu, D. R. Hedgepeth, L. Xu, and X. Tan, "A framework for modeling steady turning of robotic fish," in *Proc. IEEE Int. Conf. Robot. Autom.*, Kobe, Japan, May 2009, pp. 2669–2674.

[11] Z. Su, J. Yu, M. Tan, and J. Zhang, "Bio-inspired design of body wave and morphology in fish swimming based on linear density," in *IEEE Int. Conf. Robot. Biomim.*, Guangxi, China, Dec. 2009, pp. 1803–1808.

Appendix

A. The Rotation Transformation and Its Differentiation

As is shown in Fig. 9(a), point a rotates around point c by an angle θ, arriving at point b. It can be calculated by

$$b = \mathscr{S}_\theta(\overrightarrow{ca}) + c = \mathscr{S}_\theta(a-c) + c, \tag{19}$$

where $\mathscr{S}$ is the rotation transformation. Written in matrix form, it becomes

$$\begin{bmatrix} x_b \\ y_b \end{bmatrix} = \begin{bmatrix} \cos\theta & -\sin\theta \\ \sin\theta & \cos\theta \end{bmatrix} \begin{bmatrix} x_a - x_c \\ y_a - y_c \end{bmatrix} + \begin{bmatrix} x_c \\ y_c \end{bmatrix}. \tag{20}$$

If the angle rate is α, i.e., $\dot{\theta} = \alpha$, then we have

$$\dot{b} = (\mathscr{S}_\theta(a-c) + c)' = \mathscr{S}'_\theta(a-c), \tag{21}$$

where

$$\begin{aligned} \mathscr{S}'_\theta &= \begin{bmatrix} \cos\theta & -\sin\theta \\ \sin\theta & \cos\theta \end{bmatrix}' = \begin{bmatrix} -\sin\theta & -\cos\theta \\ \cos\theta & -\sin\theta \end{bmatrix} \cdot \dot{\theta} \\ &= \begin{bmatrix} -\sin\theta & -\cos\theta \\ \cos\theta & -\sin\theta \end{bmatrix} \cdot \alpha. \end{aligned} \tag{22}$$

If $\theta = 0$, we obtain

$$\dot{a} = \dot{b}\big|_{\theta=0} = \begin{bmatrix} 0 & -1 \\ 1 & 0 \end{bmatrix} \cdot \alpha \cdot (a-c) = \mathscr{R}_\alpha(\overrightarrow{ca}), \tag{23}$$

where $\mathscr{R}_\alpha = \begin{bmatrix} 0 & -1 \\ 1 & 0 \end{bmatrix} \cdot \alpha$ is the differentiation of the rotation transformation $\mathscr{S}$. Therefore, $\mathscr{R}_\alpha(\overrightarrow{ca})$ represents the velocity vector of point a. Similarly, (1) and (2) can be derived.

B. The Calculation of Angle Rate

From (23), we can obtain

$$|\alpha| = \frac{|\dot{a}|}{\left|\begin{bmatrix} 0 & -1 \\ 1 & 0 \end{bmatrix} \cdot \overrightarrow{ca}\right|} = \frac{|\dot{a}|}{|\overrightarrow{ca}|}. \tag{24}$$

As is shown in Fig. 9(b),the real differentiation of J_{i+1} can only be calculated by subtracting the component of $\dot{J}_{i-1}$ and $\mathscr{R}_{\alpha_{i-1}}(\overrightarrow{J_{i-1}J_{i+1}})$. Therefore, (18) is derived. Since the coordinate system is fixed on the fish head in the bending phase, so that the translation movement of J_i in Fig. 2(a) is zero. Thus, (10) is derived.